A metal-metal Fabry-Pérot cavity photoconductor for efficient GaAs terahertz photomixers

Emilien Peytavit, Christophe Coinon, Jean-Francois Lampin

A metal-metal Fabry–Pérot cavity photoconductor for efficient GaAs terahertz photomixers

Cite as: J. Appl. Phys. **109**, 016101 (2011); https://doi.org/10.1063/1.3525709
Submitted: 28 September 2010 • Accepted: 31 October 2010 • Published Online: 04 January 2011

E. Peytavit, C. Coinon and J.-F. Lampin

A metal-metal Fabry–Pérot cavity photoconductor for efficient GaAs terahertz photomixers

E. Peytavit,[a] C. Coinon, and J.-F. Lampin
UMR CNRS 8520, Institut d'Electronique, de Microélectronique et de Nanotechnologie, Avenue Poincaré, B.P. 60069, 59652 Villeneuve d'Ascq, France

(Received 28 September 2010; accepted 31 October 2010; published online 4 January 2011)

The low responsivity of the low-temperature-grown GaAs based planar photoconductors used in the photomixing experiments can be improved by using a metal-metal Fabry–Pérot cavity. This resonant cavity photoconductor exhibits a dc-responsivity above 0.1 A/W and current density higher than 50 kA/cm^2 with a low-temperature-grown-GaAs epitaxial layer presenting a subpicosecond carrier lifetime. Based on these results, up to 100 μW output power at 1 THz could be expected if this photoconductor is used in a photomixing experiment with a resonant antenna. © *2011 American Institute of Physics*. [doi:10.1063/1.3525709]

The generation of microwave radiation by mixing two laser beams on a photodetector has been shown as early as the invention of the laser.[1] Thirty years later, this technique has been successfully adapted to the terahertz (THz) range[2] with 0.8-μm-wavelength pump lasers, using an ultrafast photodetector lying at the feedpoint of a THz broadband antenna, forming a so called "photomixer." This first attempt has been carried out with a low temperature grown GaAs (LT-GaAs) planar photoconductor loaded by a silicon-lens coupled spiral antenna. Up to now, the planar photoconductor based on a short lifetime photoconductor is the most commonly used ultrafast photodetector with both 0.8-μm-wavelength and 1.55-μm-wavelength telecom pump lasers.[3–5] However, the best results around 1 THz have been achieved with a unipolar-traveling carrier photodiode[6–8] (UTC-PD) pumped by 1.5-μm-wavelength lasers. In a THz photomixing experiment, the LT-GaAs photoconductor can be modeled as a THz current source, loaded by an antenna whose impedance is supposed real (R_A), and shunted by the capacitance (C) of the metallic electrodes. The emitted THz power (P_{THz}) at a frequency f can be evaluated as follows:[2]

$$P_{THz} = \frac{1}{2} R_A \frac{|i_{THz}|^2}{1 + (2\pi f R_A C)^2}, \quad (1)$$

where $i_{THz} = i_{dc}/(1+(2\pi f \tau_c)^2)^{1/2}$ to take into account the charge carrier response time, and τ_c the carrier lifetime in the LT-GaAs. In a UTC-PD, τ_c is replaced by the transit time in the collector layer (τ_t); furthermore, there is a third cutoff frequency related to the electronic diffusion in the p-doped absorption layer. The two main advantages of the LT-GaAs planar photoconductor in comparison with the vertical-transport photodiode are (1) its lower capacitance and related $R_A C$ time constant and (2) the absence of a third cut off frequency which is essential for frequencies above 1 THz. On the other hand, i_{THz} and P_{THz} are generally lower for frequencies below 1 THz. This is mainly related to a lower i_{dc} coming from: (a) an intrinsically low responsivity defined by $\Re = i_{dc}/P_{opt}$ with P_{opt} the incident optical power; (b) the poor thermal characteristics of the LT-GaAs layer[9] which limit the maximum total heat power dissipated in the device. One way to overcome theses limits consists in using a Fabry–Pérot (FP) cavity in order to make thinner the LT-GaAs layer without decreasing the quantum efficiency of the photoconductor. Resonant enhanced photodetectors, especially 1.55 μm p-i-n-photodiodes has been widely studied in the past[10,11] with a semiconductor bragg reflector acting as back mirror. A LT-GaAs planar photoconductor with such a bragg reflector has been theoretically studied.[12] Some attempts have even been made with metallic mirrors thanks to an epitaxial-lift-off technique but with no measured photocurrent.[13] We propose in this letter a metal-metal LT-GaAs vertical cavity-resonant photoconductor (VRP), which will be studied by dc-responsivity measurements.

In Fig. 1(a) is shown a schematic of the proposed device, where the LT-GaAs photoconductor is sandwiched between two gold layers which serve at the same time as bias electrodes and optical mirrors of the FP resonator. For the generation of microwaves or THz waves, the upper bias electrode could be linked thanks to an air bridge to a thin film microstrip line ended by a microstriplike antenna such as the wideband transverse electromagnetic horn (TEM-horn) that we have developed previously[14] or a resonant patch antenna. This structure can actually be seen as a lossy FP resonator, which exhibits quantum efficiency peaks corresponding to the FP destruction interference condition, where $t_k \approx k \times \lambda/2 + \lambda/4$, $(k=0,1,2,\ldots)$ with λ the wavelength in LT-GaAs. In the case of lossless metallic mirrors, these quantum efficiency peaks reach their maximum when the reflectivity of the upper mirror R_0 is such as $R_0 = A^2$ with $(1-A)$ the absorption in a single pass in the LT-GaAs layer.[10]

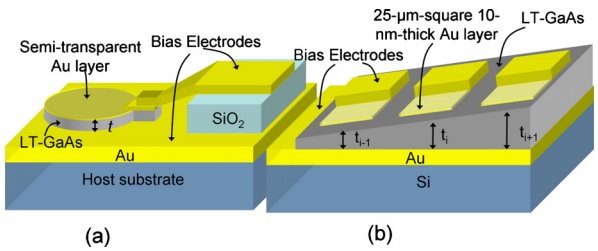

FIG. 1. (Color online) Schematic view of (a) the FP cavity photoconductor and (b) the large area photoconductors on the LT-GaAs bevel.

[a]Electronic mail: emilien.peytavit@iemn.univ-lille1.fr.

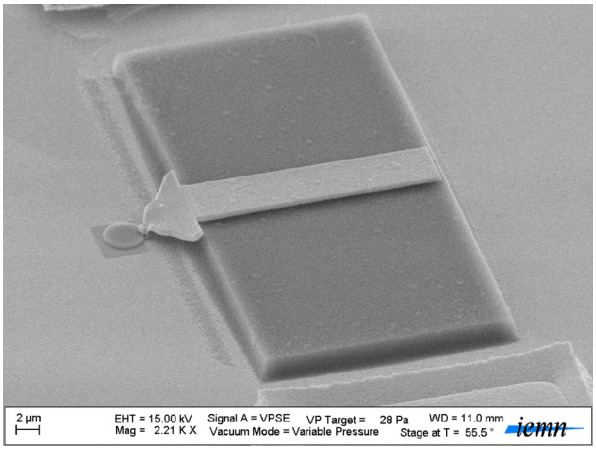

FIG. 2. (Color online) Scanning electron microscope picture of the VRP.

In order to study the VRP, two photoresponse experiments have been performed on two different samples. The first sample consists in Au–LT-GaAs–Au large area photoconductors (25-μm-square area) with various layer thicknesses (t_i) on a same epitaxial layer thanks to a bevel as shown in Fig. 1(b). In a second experiment, designed to assess the potential of this photoconductor for THz photomixing, micrometer-size photoconductors, similar to the proposed device, have been fabricated on a LT-GaAs layer of thickness $t=0.28$ μm corresponding to the third quantum efficiency peak. A scanning electron microscope picture of the device is shown in Fig. 2, where the LT-GaAs mesa can be recognized on the gold background layer, covered by a 20-nm-thick semitransparent gold layer and a 80-nm-thick Si_3N_4 layer. The semitransparent upper electrode is linked by an air-bridge to a gold strip deposited on a 2.3-μm-thick-SiO_2 layer for dc-bias by a probe-tip. Both samples were fabricated using the following procedure: starting from a 450-μm-thick semi-insulating GaAs substrate, a 0.1-μm-thick GaInP barrier was grown by gas-source molecular beam epitaxy followed by a 2-μm-thick layer for the first one and 0.28-μm-thick layer for the second one of low temperature (~200 °C) GaAs. After their growth, the samples were annealed at 580 °C for 1 min. The LT-GaAs epitaxial layers were subsequently transferred onto a 2-in.-diameter p-doped silicon wafer thanks to an Au–Au thermocompression layer transfer technique detailed in Ref. 14. Concerning the first sample, after the 2-μm-thick layer had been transferred on the gold cladded silicon substrate, a bevel etching was performed in an aqueous ammonium hydroxide and hydrogen peroxide solution. 25-μm-square area and 10-nm-thick semitransparent gold electrodes and 25-μm-square area and 20-nm-thick Ti/400-nm-thick Au contact pads were then patterned by standard microelectronic techniques in order to form the large area photoconductors. The micrometer-size photoconductors of the second sample were fabricated by using dry etching, electron-beam lithography and lift-off techniques.

The first photoresponse experiment was conducted using a distributed feedback (DFB) laser diode emitting at $hv=1.58$ eV and focused through a $f/D=1$ lens into a Gaussian spot of half-width, $w=2.5$ μm. In Fig. 3 are shown the bias voltage dependences of the photocurrents at a constant

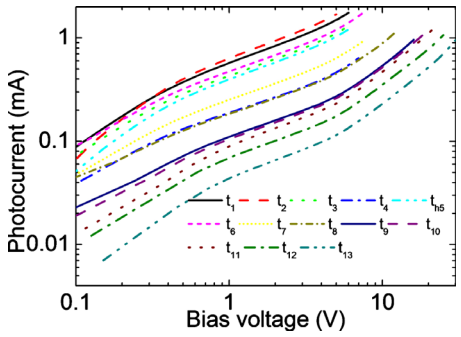

FIG. 3. (Color online) Measured photocurrent as function of bias voltage with an optical power $P_{opt}=8.9$ mW for thicknesses $t_1 \ldots t_{13}=0.25$, 0.27, 0.28, 0.31, 0.34, 0.37, 0.39, 0.50, 0.70, 0.89, 0.99, 1.10, and 1.32 μm.

optical power for layer thicknesses (t_i) between $t_1=0.25$ μm and $t_{13}=1.32$ μm. These measurements are obtained when the large area photoconductors are illuminated by an incident optical power $P_{opt}=8.9$ mW. The curves can be divided in three different parts: (1) a low voltage part, where the photocurrent increases rapidly with the bias voltage, (2) a medium voltage part with a slower increase, and (3) a last part, where occurs the so-called quadratic behavior.[15] The two first parts can be interpreted as the increases in the electron and hole photocurrents with the electric field in the mobility regime. The quadratic photocurrent, already measured in the LT-GaAs photoconductors,[15,16] appears around 5 V, whatever the layer thickness. It can be explained by a tunnel injection of carriers from the contact electrode due to an electric field peak near the anode.[17] Furthermore, it has been previously shown that this additional photocurrent has a much longer time constant than the low voltage photocurrent[15] and will be removed in the experimental data used in Fig. 4 by considering that the slope of the photocurrent curve before 5 V remains constant beyond 5 V.

In Fig. 4 are shown the theoretical (solid line) and experimental (in squares) thickness dependences of the responsivity measured for a constant mean electric field $V_{bias}/t=120$ kV/cm, close to the obscurity breakdown field in our sample. The measurement of the different layer thicknesses were achieved thanks to a profilometer with an estimated accuracy of ± 10 nm, corresponding to the width of the squares on the Fig. 4. Maxima of responsivity related to the quantum efficiency peaks clearly appear on the curves of the

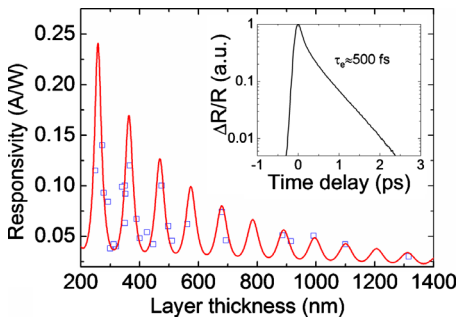

FIG. 4. (Color online) Theoretical (solid line) and experimental (in squares) reponsivities as a function of LT-GaAs layer thickness. In the inset is shown the transient differential photoreflectivity measured at $\lambda=820$ nm on the LT-GaAs layer.

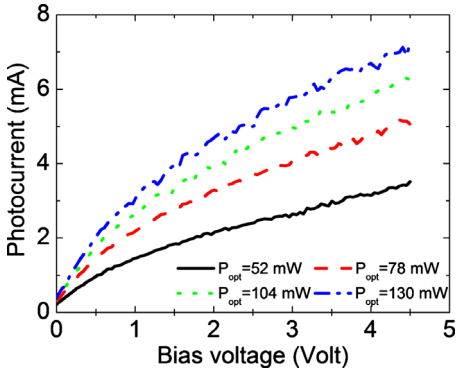

FIG. 5. (Color online) Bias voltage dependences of the photocurrent for a 4-μm-diameter photoconductor for incident optical power P_{opt}=52, 78, 104, and 130 mW.

Fig. 4, reaching values higher than 0.1 A/W when the layer thickness is smaller than 0.5 μm. In order to model this photoresponse experiment, electrons and holes are assumed to have different lifetimes, denoted, respectively, τ_e and τ_h but the same saturation velocity $v_{sat}=8\times10^6$ cm/s.[18] Under these assumptions and ignoring the effects of carrier diffusion, the responsivity $\Re$ of a carrier lifetime limited photoconductor can be written $\Re=q\eta(g_e+g_h)/h\nu$, where q is the unit electric charge, $\eta=P_{abs}/P_{opt}$ the quantum efficiency with P_{abs} the optical power absorbed in the LT-GaAs layer, $g_{e(h)}=\tau_{e(h)}/\tau_{tr}$ the electron and hole optical gains and $\tau_{tr}=t/v_{sat}$. The quantum efficiency is calculated by using a transfer matrix method, assuming an incident plane wave at normal incidence with the following optical index:[19] $n_{LT\text{-}GaAs}=3.7-i0.09$ and $n_{Au}=0.174-i4.86$. In order to estimate the carrier response time, a time-resolved photoreflectance experiment has been performed on the LT-GaAs layer after epitaxial transfer (shown in the inset of Fig. 4). After a very fast decrease during the firsts 500 fs related to the cooling and the relaxation of the carriers,[20] the differential photoreflectivity decreases exponentially with a time constant $\tau_e\approx500$ fs, which is interpreted as the lifetime of the electrons[20] in the conduction band. We obtained a similar electron lifetime ($\tau_e\approx480$ fs) on the second sample. The last parameter $\tau_h=1$ ps has been used as fit parameter and is consistent with longer hole trapping time measurement done in previous works.[21]

In the second photoresponse experiment, the incident beam comes from a continuous wave titane-saphire laser at $h\nu=1.59$ eV and is focused into a Gaussian spot of half-width $w=4$ μm. The photocurrents measured on a 4-μm-diameter photoconductor of the second sample as a function of bias voltage are plotted on the Fig. 5. The photocurrent curves have the same behavior as in the previous experiment. A photocurrent of about 7.3 mA is achieved at 4.5 V and $P_{opt}=130$ mW, i.e, a current density reaching 57 kA/cm^2, more than ten times the current density measured in a planar photoconductor.[15] It can be noted that only 40% of the incident light is coupled in the 4-μm-diameter photoconductor due to the 8-μm-spot-width beam.

In order to evaluate the THz output power achievable with this photoconductor used as photomixer, we consider that about 33% of the dc-photocurrent is related to the electrons, whose response time is $\tau_e\approx480$ fs, and 66% is related to the holes, whose response time is given by the previous experiment $\tau_h\approx1$ ps. These proportions come directly from the previous assumptions, in which electrons and holes have the same drift-velocity (v_{sat}). The electrical capacitance of the 4-μm-diameter photoconductor ($C=5.1$ fF) is easily calculated by considering that the photoconductor is a parallel plate capacitance, with 4-μm-diameter disk-shaped electrodes separated by a 0.28-μm-thick GaAs layer. The emitted THz power achievable is also dependent on the antenna impedance. A wide-band antenna such as the TEM-horn has an almost purely real radiation impedance, which is close to 50 Ω in the whole THz range. Using Eq. (1) at $f=1$ THz, the emitted THz power would be $P_{THz}\approx8$ μW. If the antenna is a narrow-band resonant antenna, the parasitic capacitance can be cancelled around the central frequency[22] by an impedance matching technique. Furthermore, the radiation impedance of the antenna could reach several hundreds ohms at the resonant frequency. For example, if $f=1$ THz is the central frequency and $R_A=200$ Ω, P_{THz} would reach about 100 μW. These results would represent a major improvement in the output THz power provided by photomixers based on 0.8-μm-wavelength as well as 1.55-μm-wavelength laser sources.

This work was supported by the CNRS and by the "Région Nord Pas de Calais."

[1] M. DiDomenico, Jr., R. H. Pantell, O. Svelto, and J. N. Weaver, Appl. Phys. Lett. **1**, 77 (1962).
[2] E. R. Brown, K. A. McIntosh, K. B. Nichols, and C. L. Dennis, Appl. Phys. Lett. **66**, 285 (1995).
[3] M. Sukhotin, E. R. Brown, A. C. Gossard, D. Driscoll, M. Hanson, P. Maker, and R. Muller, Appl. Phys. Lett. **82**, 3116 (2003).
[4] J. Mangeney, A. Merigault, N. Zerounian, P. Crozat, K. Blary, and J. F. Lampin, Appl. Phys. Lett. **91**, 241102 (2007).
[5] M. Mikulics, M. Marso, I. Camara Mayorga, R. Gusten, S. Stancek, P. Kovac, S. Wu, X. Li, M. Khafizov, R. Sobolewski, E. A. Michael, R. Schieder, M. Wolter, D. Buca, A. Forster, P. Kordos, and H. Luth, Appl. Phys. Lett. **87**, 041106 (2005).
[6] H. Ito, F. Nakajima, T. Furuta, K. Yoshino, Y. Hirota, and T. Ishibashi, Electron. Lett. **39**, 1828 (2003).
[7] F. Nakajima, T. Furuta, and H. Ito, Electron. Lett. **40**, 1297 (2004).
[8] E. Rouvalis, C. Renaud, D. Moodie, M. Robertson, and A. Seeds, Opt. Express **18**, 11105 (2010).
[9] A. W. Jackson, J. P. Ibbetson, A. C. Gossard, and U. K. Mishra, Appl. Phys. Lett. **74**, 2325 (1999).
[10] J. Farhoomand and R. E. McMurray, Jr., Appl. Phys. Lett. **58**, 622 (1991).
[11] M. S. Ünlü and S. Strite, J. Appl. Phys. **78**, 607 (1995).
[12] E. R. Brown, Appl. Phys. Lett. **75**, 769 (1999).
[13] B. Corbett, L. Considine, S. Walsh, and W. M. Kelly, Electron. Lett. **29**, 2148 (1993).
[14] E. Peytavit, J.-F. Lampin, F. Hindle, C. Yang, and G. Mouret, Appl. Phys. Lett. **95**, 161102 (2009).
[15] E. R. Brown, K. A. McIntosh, F. W. Smith, K. B. Nichols, M. J. Manfra, C. L. Dennis, and J. P. Mattia, Appl. Phys. Lett. **64**, 3311 (1994).
[16] S. M. Duffy, S. Verghese, and K. A. McIntosh, in *Sensing with Terahertz Radiation*, edited by D. Mittelman (Springer, Berlin, 2003), p. 193.
[17] S. E. Ralph and D. Grischkowsky, Appl. Phys. Lett. **59**, 1972 (1991).
[18] E. Y. Wu and B. H. Yu, Appl. Phys. Lett. **58**, 1503 (1991).
[19] *Handbook of Optical Constants of Solids*, edited by E. D. Palik (Academic, New York, 1998).
[20] M. Stellmacher, J. Nagle, J. F. Lampin, P. Santoro, J. Vaneecloo, and A. Alexandrou, J. Appl. Phys. **88**, 6026 (2000).
[21] R. Adomavičius, A. Krotkus, K. Bertulis, V. Sirutkaitis, R. Butkus, and A. Piskarskas, Appl. Phys. Lett. **83**, 5304 (2003).
[22] S. M. Duffy, S. Verghese, A. McIntosh, A. Jackson, A. C. Gossard, and S. Matsuura, IEEE Trans. Microwave Theory Tech. **49**, 1032 (2001).